Doping and photo-induced i.r. absorption spectrum of *trans* polyacetylene

P. Piaggio and G. Dellepiane
Istituto di Chimica Industriale dell'Università, 16100 Genova, Italy

and E. Mulazzi
Dipartimento di Fisica, Università di Milano and GNSM, via Celoria 16, 20133 Milano, Italy

and R. Tubino
Istituto di Chimica delle Macromolecole del CNR, via Bassini 15, 20133 Milano, Italy
(Received 26 August 1986; accepted 17 November 1986)

Doping induced i.r. absorption spectra of samples of various conjugation lengths, both in solution and in the solid phase, have been measured. A well defined and striking correlation between the positions of the absorption peaks centred at about $\omega \sim 900\,cm^{-1}$ and at $\omega \sim 1415\,cm^{-1}$ and the number of conjugated double bonds has been observed. A theoretical model based on the perturbed Green function formalism, which includes the phonon frequency dispersion and the change of the phonon frequencies with the segment conjugation length, accounts for the present experimental data as well as for the features of the photoinduced spectrum.

(Keywords: photoexcitation; conducting polymer; *trans* polyacetylene; i.r. spectra; doping)

INTRODUCTION

The investigation of the properties of photo-induced[1] i.r. and the doping induced i.r. spectra[2,3] in *trans* $(CH)_x$ and $(CD)_x$ has recently been the subject of much experimental interest. In fact from the understanding of these i.r. features, one can obtain more information on the conductivity and photoconductivity mechanism in the *trans* polyacetylene polymer.

The main features of the photo-induced i.r. spectrum are extensively discussed in ref. 1 and from the spectra recorded there one can observe the vibrational bands peaked at $\omega_{1H} \simeq 500\,cm^{-1}$, $\omega_{2H} \simeq 1270\,cm^{-1}$, $\omega_{3H} \simeq 1370\,cm^{-1}$ in *trans* $(CH)_x$ and $\omega_{1D} \simeq 400\,cm^{-1}$, $\omega_{2D} \simeq 1045\,cm^{-1}$, $\omega_{3D} \simeq 1225\,cm^{-1}$ in *trans* $(CD)_x$, respectively. In order to interpret these results, it is important to recall that the i.r. absorption technique probes the response of the whole system and it is not sensitive to selective excitation wavelengths like Resonant Raman Scattering (RRS) experiments. However, from the RRS spectra one can deduce that in good quality *trans* polyacetylene samples the chains are constituted by a majority of long segments[4,5]. So one can expect that the photo-induced i.r. response is mainly determined by the new vibrational modes of long segments, perturbed by the photogenerated charges in the excited states.

Measurements of the doping induced i.r. spectra performed on the doped *trans* $(CH)_x^2$ and *trans* $(CD)_x^3$ samples show that the vibrational peaks are at $\omega_{1H} \simeq 880\,cm^{-1}$, $\omega_{2H} \simeq 1280\,cm^{-1}$ and $\omega_{3H} \simeq 1400\,cm^{-1}$; $\omega_{1D} \simeq 790\,cm^{-1}$, $\omega_{2D} \simeq 1110\,cm^{-1}$ and $\omega_{3D} \simeq 1240\,cm^{-1}$, respectively. Notice that ω_{1H} and ω_{3H} are displaced with respect to those of the photo-induced case and that the relative bands are more intense and wider. Such different results can be interpreted in terms of the different perturbation induced by the dopant into the system. In fact from the RRS spectra from the doped samples[6], one can deduce that a broad distribution of short segment is present in the doped *trans* polyacetylene systems. Then the results reported in refs. 2 and 3 can be explained by considering the dynamical properties of different conjugated segments and in particular the short segments perturbed by the dopant.

In this paper we report the doping induced i.r. spectra from samples of *trans* polyacetylene chains constituted by segments of differing conjugated lengths. In particular we have studied the dependence of the frequency position of the peaks of the doping induced i.r. bands on the average conjugated length of the segments. We present also an interpretation of the experimental results by using the perturbed Green function method which can account for the features of the photo-induced i.r. spectra[7] and those of the doping induced i.r. spectra.

EXPERIMENTAL RESULTS

The recent availability of samples of polyacetylene of controlled conjugation length, obtained by grafting polyenic chains to polybutadiene as described in ref. 8, provides new information on the dependence of the spectroscopical properties on the average length of the conjugated segments. This allows us to investigate the dependence of the peak position of electronic absorption spectrum and of the doping induced i.r. bands, on the extent of the π electron delocalization.

In *Figure 1* we show the electronic absorption spectrum of graft $(CH)_x$. The position of the absorption maximum of sample (A) is typical of *trans* conjugated segments of

0032-3861/87/040563-04$03.00

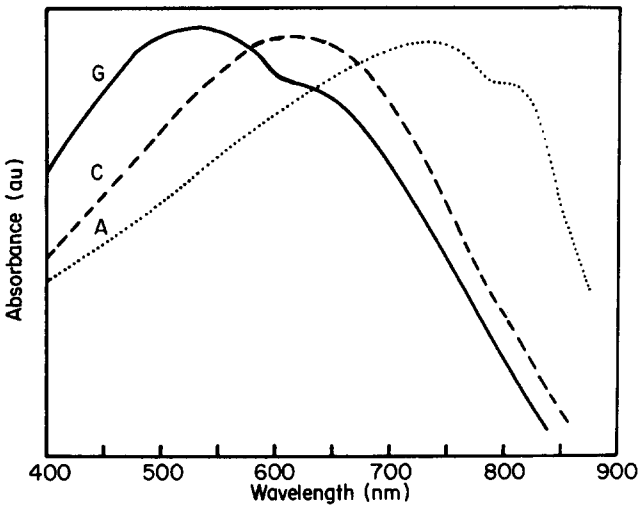

Figure 1 Electronic absorption spectra of samples of graft *trans* $(CH)_x$ with different average conjugation lengths

high conjugation length[9]. On the other hand, sample (G) exhibits a spectrum considerably blue shifted typical of short conjugated sequences. An intermediate behaviour is observed for sample (C). In all these samples the considerable width of the absorption is indicative of a distribution of segments of different conjugated length. In *Figure 2* we report the doping induced i.r. bands for samples of decreasing conjugated length sequences (A–G). All the spectra were measured under the same experimental conditions at low doping levels. The dip observed at $1010\,cm^{-1}$ in all the spectra is possibly due to a lack of compensation of the strong CCH out of plane bending of the pristine polymer. As an alternative explanation the dip is due to a true absorption originating from the doping of the segments of very short conjugated length.

From *Figure 2* it is possible to observe that while the position of the weak band at $\sim 1290\,cm^{-1}$ does not change with the sample, the two strong bands at $\sim 900\,cm^{-1}$ and $\sim 1400\,cm^{-1}$ exhibit a systematic variation with the average conjugation length of the sequences present in the sample. Moreover the complex shape of the $900\,cm^{-1}$ band shows drastic changes. From *Figure 2* it is possible to deduce, going from (A) to (G), that both these bands shift appreciably toward higher frequencies as the average length of the conjugated sequences is lowered.

In *Figure 3* we show the plot of $\omega_{3H}(\omega \sim 1400\,cm^{-1})$ *versus* $\omega_{1H}(\omega \sim 900\,cm^{-1})$ and from the graph it is possible to deduce that an approximate linear correlation exists between the frequencies of the peak positions of these two bands which can be written as follows:

$$\omega_{3H} = 1210\,cm^{-1} + 0.207\omega_{1H} \qquad (1)$$

Equation (1) appears to reproduce quite well not only the present data on the graft $(CH)_x$ (○ in *Figure 3*), but also all the existing frequencies of the doping induced i.r. bands of samples obtained with various polymerization techniques (□, △ in *Figure 3* taken from refs. 2, 10–14).

THEORETICAL MODEL

The experimental results of the photogenerated i.r. spectrum and of the doping induced i.r. spectra shown in *Figure 2* can be accounted for by a theoretical model based on the perturbed Green function method.

We start by applying the formalism in order to compute the photo-induced i.r. frequencies and their relative integrated intensities to be compared with the experimental results.

As we pointed out before, since the chains of good quality samples are mainly constituted by long segments[4,5], the photo-induced i.r. spectrum is determined mainly by the new vibrational modes of these segments, which are perturbed by the photogenerated charges.

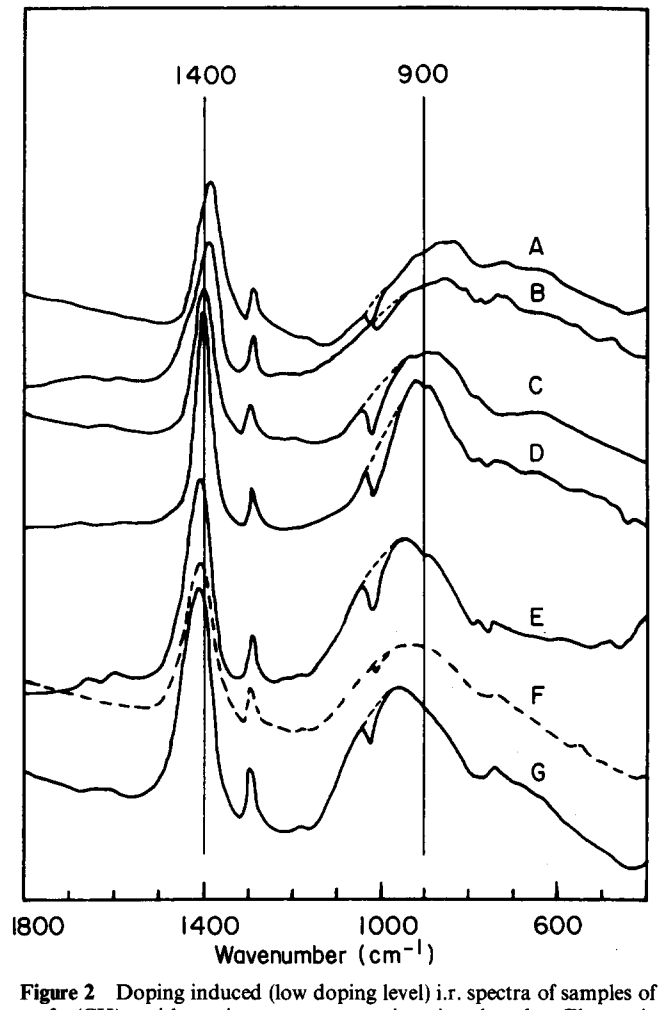

Figure 2 Doping induced (low doping level) i.r. spectra of samples of graft $(CH)_x$ with various average conjugation lengths. Electronic characterizations of the samples (A), (C) and (G) are reported in *Figure 1*. Doping agent is I_2 except for sample F, which has been doped with Br_2

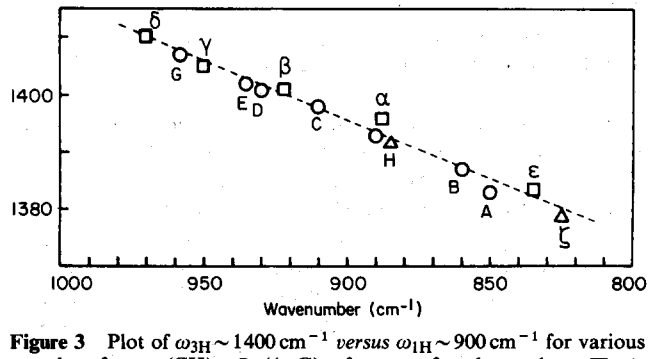

Figure 3 Plot of $\omega_{3H} \sim 1400\,cm^{-1}$ *versus* $\omega_{1H} \sim 900\,cm^{-1}$ for various samples of *trans* $(CH)_x$. ○ (A–G) refer to graft polyacetylene; □, △ solid samples (α–ζ from refs 2 and 10–14; (H) Shirakawa film, unpublished data)

Then we use a lattice dynamical model to describe the vibrational properties of *trans* polyacetylene in the unperturbed ground state, based on the following assumptions:

(i) The sample is constituted primarily by long segments with cyclic boundary conditions.
(ii) The dimerization properties are properly taken into account by using appropriate force constants, redefined in terms of a detailed study of the electron phonon interactions[15].
(iii) The effects of the photogenerated charges on the lattice dynamics are described by a force constant perturbation $\Lambda(\omega^2)$, which is due to the change of the screened electron–electron interaction and of the electron phonon interaction in the excited states.

Following the treatment of ref. 16 we can write that the perturbed Green function $G(\omega^2+i0^+)$ is given by

$$G(\omega^2+i0^+) = (1-G^\circ(\omega^2+i0^+)\Lambda(\omega^2))^{-1}G^\circ(\omega^2+i0^+) \quad (2)$$

where $G^\circ(\omega^2+i0^+)$ is the unperturbed Green function in the ground state.

We can write the perturbed density of vibrational states in the excited electronic states in the following way:

$$\rho(\omega^2)=\frac{\rho^\circ(\omega^2)}{|1-\tilde{\rho}^\circ(\omega^2)\Lambda(\omega^2)|^2+|\pi\rho^\circ(\omega^2)\Lambda(\omega^2)|^2} \quad (3)$$

where $\rho^\circ(\omega^2)=(1/\pi)\mathrm{Im}\ G^\circ(\omega^2+i0^+)$

$$\tilde{\rho}^\circ(\omega^2)=P\int 2\omega'\,\mathrm{d}\omega'\left(\frac{1}{\omega^2-\omega'^2}\right)\rho^\circ(\omega'^2) \quad (4)$$

The new vibrational modes with frequencies ω_i $(i=1,2,3)$ are determined by the zeros of the following equation

$$\frac{1}{\Lambda(\omega^2)}=\tilde{\rho}^\circ(\omega) \quad (5)$$

The integrated intensity of the new modes at frequency ω_i are given by[16]:

$$I(\omega_i)\propto|\Lambda(\omega_i^2)\tilde{\rho}^{\circ\prime}(\omega_i^2)|^{-1} \quad (6)$$

$\tilde{\rho}^{\circ\prime}(\omega^2)$ is the derivative of $\tilde{\rho}^\circ(\omega^2)$ and is evaluated at the frequency ω_i. In the approximation used to compute $\rho(\omega^2)$, we take into account the dispersion relationship of the vibrational modes by fitting in an analytical way the results of ref. 15. The effect of the negative charges in the excited states determines a positive change of the force constant in the dynamical matrix. For this reason the perturbation Λ can only have positive values.

In *Figure 4* we plot $\tilde{\rho}^\circ(\omega^2)$ for *trans* $(CH)_x$ as a function of ω following equation (4). The new vibrational frequencies, which are the poles of equation (3) are obtained as the roots of equation (5). In *Table 1* we list the calculated frequencies ω_i and the integrated intensities to be compared with the experimental values.

Examination of *Table 1* and *Figure 4* shows that the integrated intensity of ω_{1H} is always larger than that for ω_{3H} and ω_{2H} independently of the change of the force constant. The value of Λ is expected to be influenced by the detailed behaviour of the photogenerated charges on the long segments and can modify ω_{1H} at larger extent than ω_{3H}, while ω_{2H} is almost unaffected. This effect could

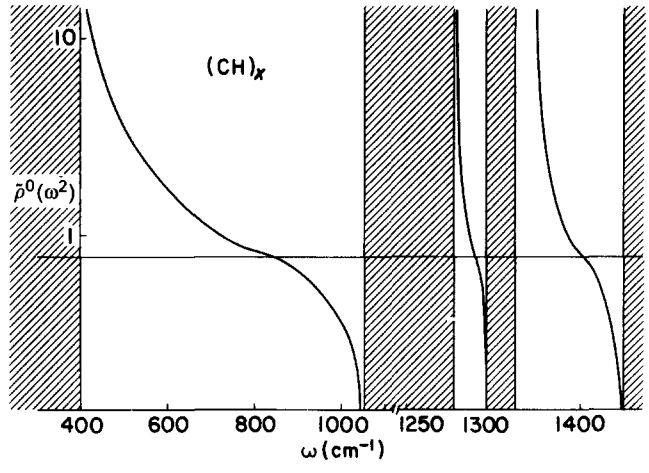

Figure 4 Calculated $\tilde{\rho}^\circ(\omega^2)$ as function of ω for *trans* $(CH)_x$. Note the change of scale in the intervals 1100–1200 cm^{-1} and 1200–1450 cm^{-1}. The values of $\tilde{\rho}^\circ(\omega^2)$ are given in 10^{-6} cm^2

Table 1 Experimental and calculated i.r. photoinduced frequencies. $\bar{\Lambda}$ refers to the selected change of the force constant in order to fit the experimental data. $I(\omega_i)/I(\omega_1)$ is the ratio between the integrated intensity of the bands peaked at ω_i $(i=1,2,3)$ and that at ω_1

	Photoinduced i.r. frequencies		
	Experimental[1] cm^{-1}	Theoretical cm^{-1} ($\bar{\Lambda}=1.7\times10^6$ cm^{-2})	$\frac{I(\omega_i)}{I(\omega_1)}$
ω_{1H}	500	510	1
ω_{2H}	1275	1270	0.02
ω_{3H}	1365	1360	0.7
ω_{1D}	400	420	1
ω_{2D}	1045	1045	0.5
ω_{3D}	1225	1225	0.02

account for the band shapes of the three photogenerated bands; for the discussion about this point see ref. 7.

In order to calculate the doping induced i.r. spectrum, it is possible to follow the same treatment as indicated before. The dopant induces a larger perturbation on the lattice force constant, then in order to find the new vibrational modes, Λ which is always positive, becomes of the order of 30×10^6 cm^{-2}. In this way it is possible to find that the new poles of equation (3) are at $\omega_{1H}=850\,cm^{-1}$, $\omega_{2H}=1279\,cm^{-1}$, $\omega_{3H}=1400\,cm^{-1}$ (see *Figure 4*). These values turn out to be in agreement with the frequencies at the peaks of the bonds shown in *Figure 2(A)*.

In order to account for the doping induced spectra and the band shapes shown in *Figure 2*, one has to consider also the effect of the dopant on short segments. In a similar way as we have done for long segments, we have treated the vibrational properties of the doping induced i.r. modes of short sequences. Since ω_{1H} is more sensitive to any change in Λ than all other doping induced frequencies, we plot the calculated values of ω_{1H} as function of Λ in *Figure 5*. Notice that curve (A) refers to ω_{1H} values for long segments and curve (B) for short segments. By considering that Λ changes in the different samples and by taking into account a distribution of Λ, due to a detailed behaviour of the doping induced charges on long and short segments, one can obtain a distribution of frequencies which can simulate the band shapes of ω_{1H}

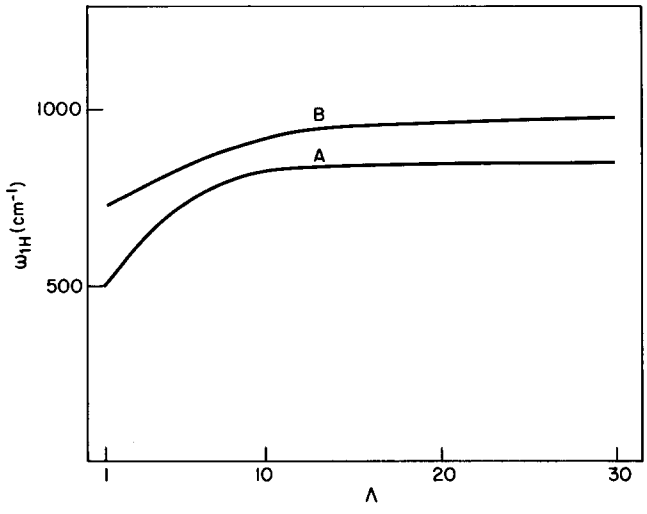

Figure 5 Calculated ω_{1H} *versus* Λ (given in 10^6 cm^{-2} units): curve (A) refers to lattice dynamical calculation for long segments; curve (B) refers to lattice dynamical calculation for short segments

reported in *Figure 2* for different samples. In particular for $\Lambda = 30 \times 10^6$ cm^{-2} the values of the new frequencies in short segments are $\omega_{1H} = 980$ cm^{-1}, $\omega_{2H} = 1279$ cm^{-1}, $\omega_{3H} = 1420$ cm^{-1}. These values are in good agreement with the frequencies at the peaks of the bands shown in *Figure* 2(*G*). From the calculated frequencies for ω_{iH}, it is possible to conclude that ω_{1H} is changing in a more dramatic way than ω_{3H}, while the value of ω_{2H} is almost unaffected by the change of Λ and by changing the distribution of long and short segments in the samples. This result can account for the phenomenological law given in equation (1).

ACKNOWLEDGEMENTS

This work has been partly supported by Progetto Finalizzato Chimica Fine Secondaria del CNR. One of us (E.M.) acknowledges also the partial support from the Nato Research Grant No. 425/84.

REFERENCES

1 Blanchet, G. B., Fincher, C. R., Chung, T. C. and Heeger, A. J. *Phys. Rev. Lett.* 1983, **50**, 1938; Shaffer, H. and Heeger, A. J. to be published
2 Harada, I., Furukawa, Y., Tasumi, M., Shirakawa, H. and Ikeda, S. *J. Chem. Phys.* 1978, **73**, 4746
3 Takeuchi, H., Furukawa, Y., Harada, I. and Shirakawa, H. *J. Chem. Phys.* 1984, **80**, 2925
4 Brivio, G. P. and Mulazzi, E. *Chem. Phys. Lett.* 1983, **95**, 555; Brivio, G. P. and Mulazzi, E. *Phys. Rev. B* 1984, **30**, 876
5 Tiziani, R., Brivio, G. P. and Mulazzi, E. *Phys. Rev. B* 1985, **31**, 4015
6 Lefrant, S., Faulques, E., Brivio, G. P. and Mulazzi, E. *Solid State Comm.* 1985, **53**, 583
7 Brivio, G. P. and Mulazzi, E. to be published in *Solid State Comm.* 1986
8 Destri, S., Catellani, M. and Bolognesi, A. *Makromol. Chem. Rapid Commun.* 1984, **5**, 353
9 Eckardt, H. *Solid State Comm.* 1985, **55**, 1075
10 Francois, B., Bernard, M. and André, J. J. *J. Chem. Phys.* 1981, **75**, 4142
11 Yaniger, S. I., Riseman, S. M., Friga, T. and Eyring, E. M. *J. Chem. Phys.* 1982, **76**, 4298
12 Clarke, T. C., McQuillan, B. W., Rabolt, J. F., Scott, J. C. and Street, G. B. *Mol. Cryst. Liq. Cryst.* 1982, **83**, 1033
13 Rabolt, J. F., Clarke, T. C. and Street, G. B. *J. Chem. Phys.* 1979, **71**, 4614
14 Piaggio, P., Dellepiane, G., Piseri, L., Tubino, R. and Taliani, C. *Solid State Comm.* 1984, **50**, 947
15 Piseri, L., Tubino, R., Paltrinieri, L. and Dellepiane, G. *Solid State Comm.* 1983, **46**, 183
16 Mulazzi, E., Nardelli, G. F. and Terzi, N. *Phys. Rev.* 1968, **42**, 847